

KEY RESOURCES TABLE

| REAGENT or RESOURCE | SOURCE | IDENTIFIER |
|--|------------------|--------------------------------|
| Antibodies | | |
| Mouse monoclonal anti-TUJ1 | Santa Cruz | Cat#sc-5274; RRID: AB_2288090 |
| Rabbit polyclonal anti-MAP2 | CST | Cat#4542s; RRID: AB_10693782 |
| Mouse monoclonal anti-NEUN | Millipore | Cat#MAB377; RRID: AB_2298772 |
| Rabbit monoclonal anti-Choline | Abcam | Cat#ab181023; RRID: AB_2687983 |
| Rabbit polyclonal anti-vGLUT1 | Synaptic Systems | Cat#135302; RRID: AB_887877 |
| Rabbit monoclonal anti-GAD67 | Abcam | Cat#ab213508 |
| Rabbit monoclonal anti-TH | Abcam | Cat#ab137869; RRID: AB_2801410 |
| Mouse monoclonal anti-GFAP | Millipore | Cat#MAB360; RRID: AB_11212597 |
| Mouse monoclonal anti-Vimentin | Santa Cruz | Cat#sc-32322; RRID: AB_628436 |
| Alexa Fluor 488 Donkey Anti-mouse | Abcam | Cat#ab150109; RRID: AB_2571721 |
| Alexa Fluor 555 Donkey Anti-rabbit | Abcam | Cat#ab150074; RRID: AB_2636997 |
| Chemicals, Peptides, and Recombinant Proteins | | |
| Forskolin | Selleck | S2449; CAS: 66575-29-9 |
| cAMP | Sigma-Aldrich | 20-198 |
| 8-Bromo-cAMP | Selleck | S7857; CAS: 76939-46-3 |
| SP600125 | Selleck | S1460; CAS: 129-56-6 |
| LDN-193189 | Selleck | S2618; CAS: 1062368-24-4 |
| Recombinant Human FGF-basic (bFGF) | Peprtech | Cat#100-18B |
| Recombinant Human BDNF | Peprtech | Cat#450-02 |
| Recombinant Human GDNF | Peprtech | Cat#450-10 |
| Recombinant Human NT-3 | Peprtech | Cat#450-03 |
| Critical Commercial Assays | | |
| RNA isolater Total RNA Extraction Reagent | Vazyme | Cat#R401-01 |
| HiScript III RT SuperMix for qPCR kit | Vazyme | Cat#R323-01 |
| ChamQ SYBR qPCR Master Mix kit | Vazyme | Cat. #Q711-02 |
| Deposited Data | | |
| RNA-seq data | This paper | GEO: GSE206514 |
| ScRNA-seq data | This paper | GEO: GSE206766 |

| | | |
|---|------------|----------------|
| ScATAC-seq data | This paper | GEO: GSE206767 |
| Experimental Models: Cell Lines | | |
| BJ cells | ATCC | CRL-2522 |
| Oligonucleotides | | |
| Primer: GAPDH Forward: TCCTGCACCACCAACTGCTT | This paper | N/A |
| Primer: GAPDH Reverse: ACCATGAGTCCTTCCACGAT | This paper | N/A |
| Primer: TUJ1 Forward: GCAACTACGTGGGCGACT | This paper | N/A |
| Primer: TUJ1 Reverse: CGAGGCACGTACTTGTGAGA | This paper | N/A |
| Primer: DCX Forward: CAAGTCTAAGCAGTCTCCATC | This paper | N/A |
| Primer: DCX Reverse: ATAGCCCTGTTGGACACTTG | This paper | N/A |
| Primer: MAP2 Forward: CAGGAGACAGAGATGAGAATTCC | This paper | N/A |
| Primer: MAP2 Reverse: CAGGAGTGATGGCAGTAGAC | This paper | N/A |
| Primer: SYN1 Forward: CCCCAATCACAAGAAATGCTC | This paper | N/A |
| Primer: SYN1 Reverse: ATGTCCTGGAAGTCATGCTG | This paper | N/A |
| Primer: COL1A1 Forward: GAGGGCCAAGACGAAGACATC | This paper | N/A |
| Primer: COL1A1 Reverse: CAGATCACGTCATCGCACAAAC | This paper | N/A |
| Primer: CTGF Forward: CATCTCCACCCGGGTTACCAA | This paper | N/A |
| Primer: CTGF Reverse: AGTACGGATGCACTTTTTGC | This paper | N/A |
| Primer: THY1 Forward: ATCGCTCCTGCTAACAGTC | This paper | N/A |
| Primer: THY1 Reverse: CTCGTACTGGATGGGTGAACT | This paper | N/A |
| Primer: DKK3 Forward: CTGGGAGCTAGAGCCTGATG | This paper | N/A |
| Primer: DKK3 Reverse: TCATACTCATCGGGGACCTC | This paper | N/A |
| Primer: CREB1 Forward: TGTAAGTATTCCAAAAGCG | This paper | N/A |
| Primer: CREB1 Reverse: TCTTCTTCAATCCTTGGCACT | This paper | N/A |
| Primer: MAPK8 Forward: GACGACGCGGCTTGATT | This paper | N/A |
| Primer: MAPK8 Reverse: TAAGGCTGCAAGACCGGC | This paper | N/A |
| Software and Algorithms | | |

| | | |
|------------------|--|---|
| GraphPad Prism 9 | GraphPad Software | https://www.graphpad.com/ |
| ImageJ | NIH | https://imagej.nih.gov/ij/download.html |
| R version 4.0.5 | The R Foundation for Statistical Computing | https://www.r-project.org/ |

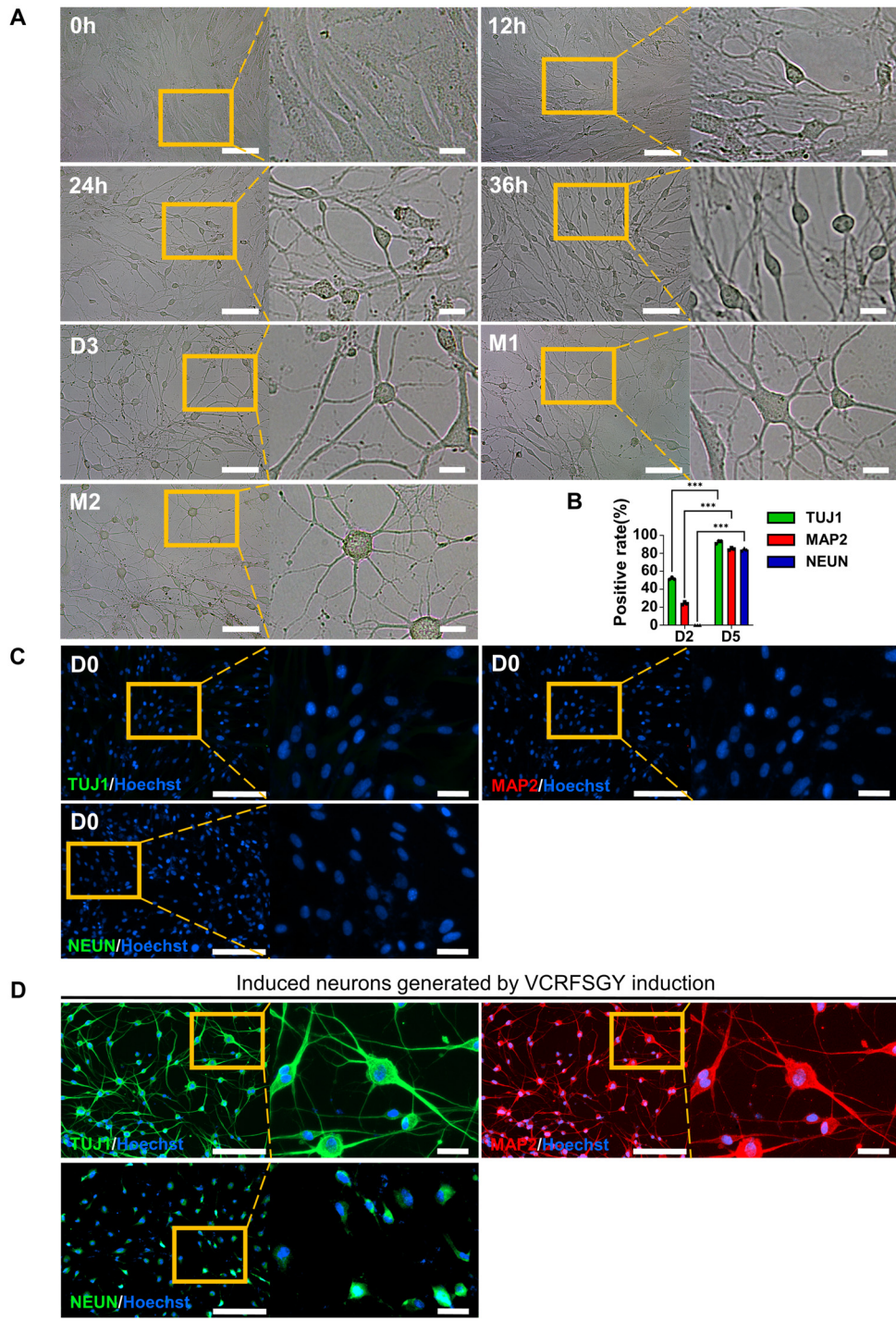


Figure S1. Morphological changes in induced cells from the BJ cell stage to two months post-induction and immunofluorescence staining for TUJ1, MAP2, and NEUN.

A. Brightfield and regional magnification of forskolin (F) induction at 0, 12, 24 and 36 h; 1 month (M1); and 2 months (M2). Scale bars, 100 μm . Magnification scale bars, 20 μm .

B. Statistical chart of the changes in TUJ1-, MAP2-, and NEUN-positive rates in cells induced with forskolin for 2 days and 5 days (mean \pm SEM, n=3 biological replicates, ***p < 0.001, one-way ANOVA).

C. BJ cells (day 0) stained negative for the neuronal markers TUJ1, MAP2 and NEUN and were used as negative controls. Scale bars, 200 μm . Magnification scale bars, 40 μm .

D. Human induced neuronal cells generated from somatic cells by induction with a small molecule cocktail (VCRFSGY) as described in a previous report stained positively for TUJ1, MAP2 and NEUN and were used as positive controls. Scale bars, 200 μm . Magnification scale bars, 40 μm .

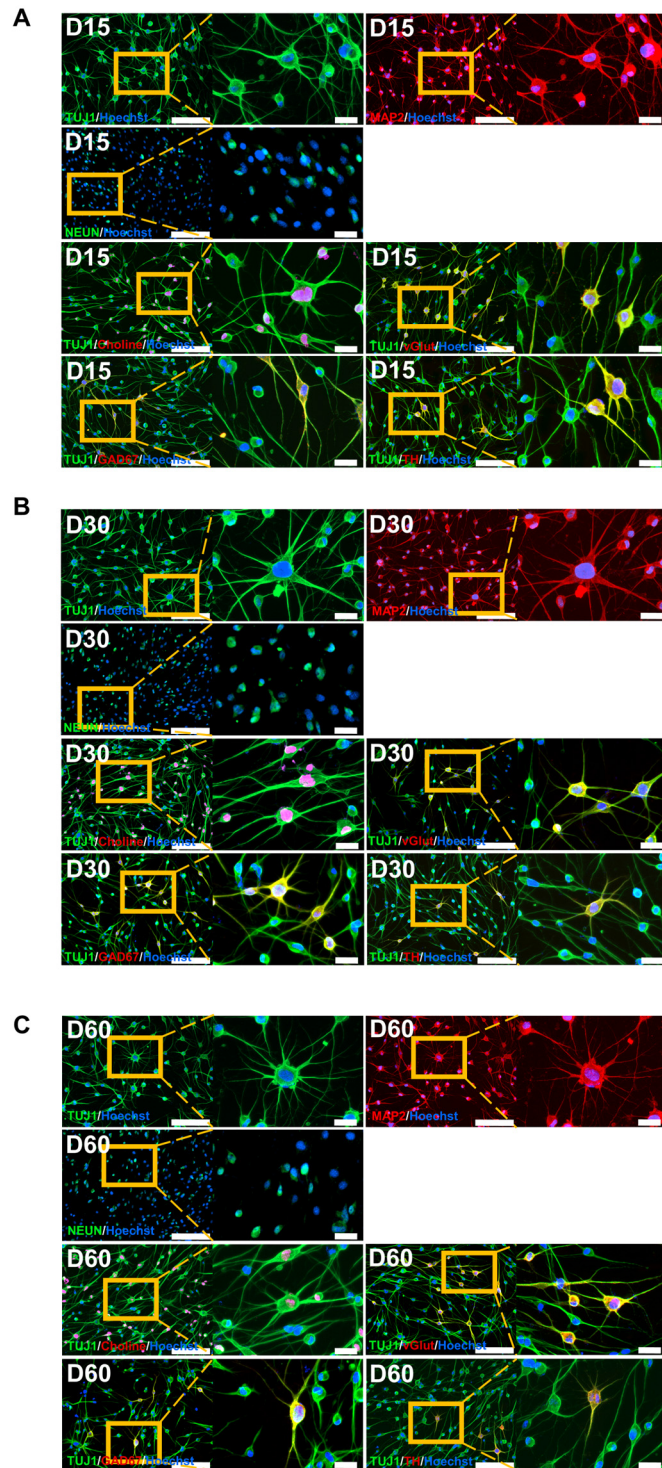


Figure S2. Immunofluorescence staining of FiNs at D15, -30, -60.

A-C. Immunofluorescence staining for neuronal markers, TUJ1 (green), MAP2 (red), NEUN (green), choline (red), vGlut (red), GAD67 (red), TH (red) and Hoechst (blue) at D15, -30, and -60. TUJ1-positive cells are shown in green. Scale bars, 200 μm . Magnification scale bars, 40 μm .

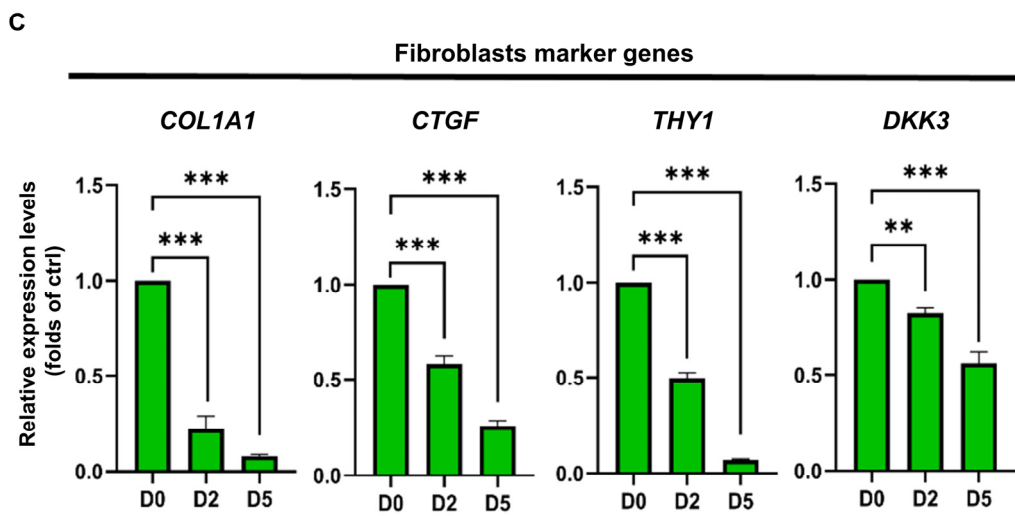
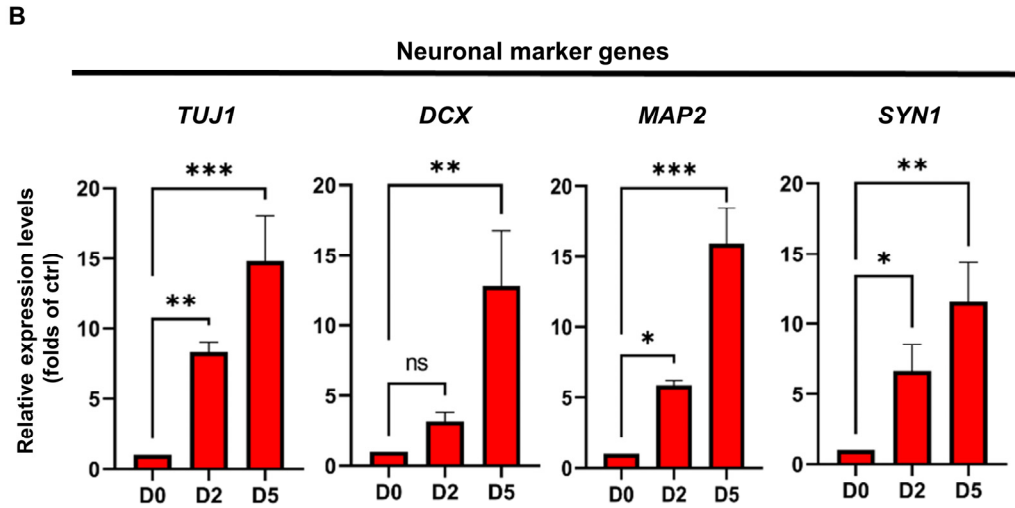
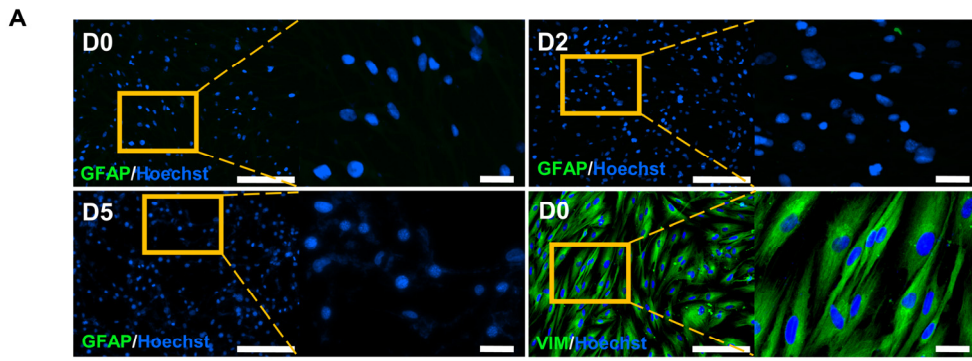


Figure S3. Immunofluorescence staining for GFAP and VIM, qRT-PCR for the expression of marker genes.

A. Cells stained negative for an astrocyte marker (GFAP) at day 0 (D0), day 2 (D2) and day 5 (D5) during forskolin induction. BJ cells (D0) stained positive for a fibroblast marker (Vimentin/VIM). Scale bars, 200 μm . Magnification scale bars, 40 μm .

B-C. qRT-PCR analysis of cells after forskolin induction for 0, 2, and 5 days (mean \pm SEM, $n=3$ biological replicates, * $p < 0.05$, ** $p < 0.01$, *** $p < 0.001$, one-way ANOVA).

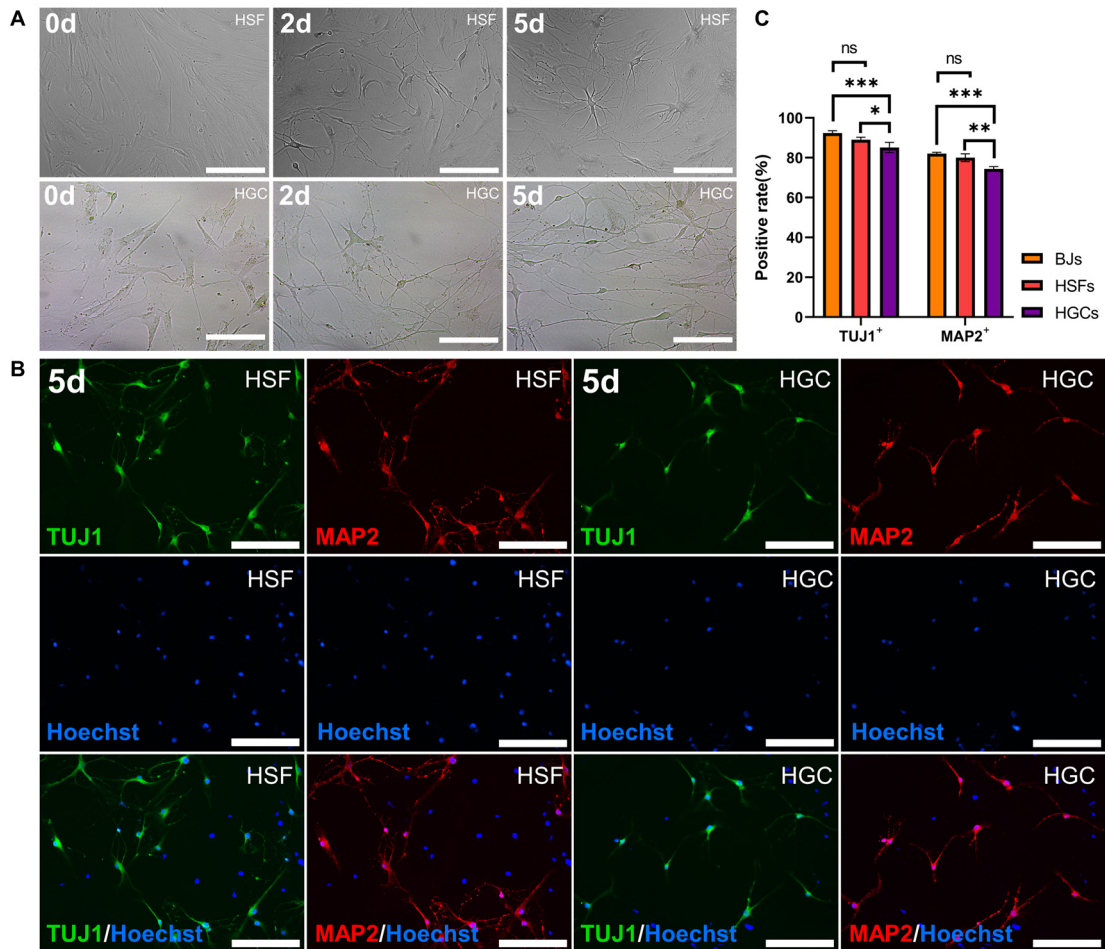


Figure S4. Human adult somatic cells (HSFs and HGCs) were converted into induced neurons under forskolin induction.

A. Morphological changes in human adult skin fibroblasts (HSFs, age 24, male) and human adult ovarian granule cells (HGCs, age 35, female) induced by forskolin at 0-, 2-, and 5 days post induction. Scale bars, 200 μ m.

B. TUJ1 (green) and MAP2 (red) immunostaining (co-staining) of induced neurons (iNs) generated from HSFs and HGCs induced by forskolin at 5 days post induction. Scale bars, 200 μ m.

C. The positive rate of TUJ1 and MAP2 immunofluorescence of iNs derived from BJ, HSFs and HGCs induced by forskolin at 5 days post induction (mean \pm SEM, n=3 biological replicates, *p < 0.05, **p < 0.01, ***p < 0.001, two-way ANOVA).

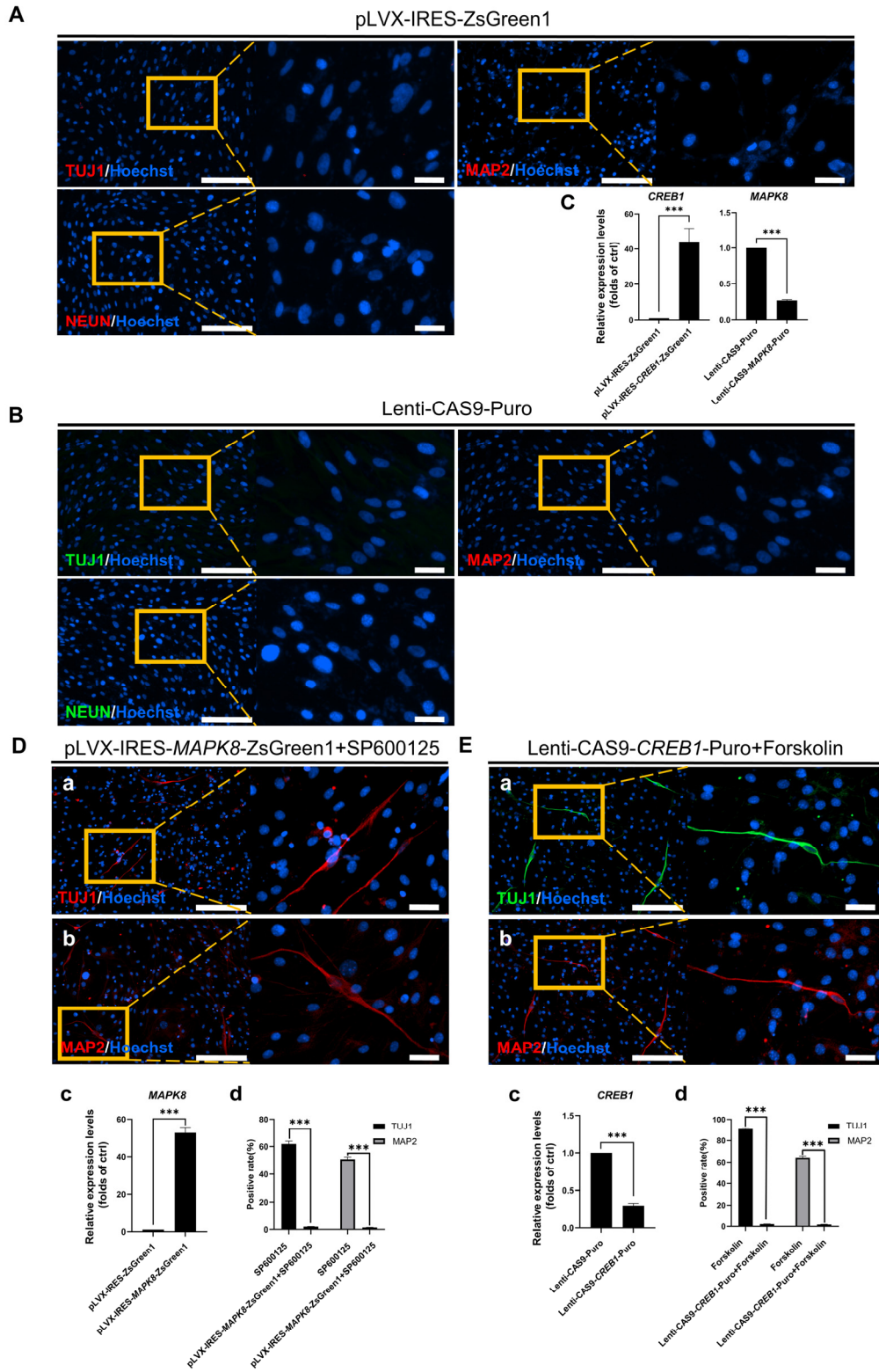


Figure S5. BJ cells transfected with pLVX-IRES-ZsGreen1 or Lenti-CAS9-Puro were negative for TUJ1, MAP2, NEUN, and *JNK (MAPK8)* overexpression or *CREB1* downregulation, which significantly interrupted SP600125 or forskolin induction, respectively.

A. BJ cells transfected with pLVX-IRES-ZsGreen1 (empty vector) stained negative for the neuronal markers TUJ1 (red), MAP2 (red), and NEUN (red) and were used as negative controls. Scale bars, 200 μm . Magnification scale bars, 40 μm .

B. BJ cells transfected with Lenti-CAS9-Puro (empty vector) stained negative for the neuronal markers TUJ1 (green), MAP2 (red), and NEUN (green) and were used as negative controls. Scale bars, 200 μm . Magnification scale bars, 40 μm .

C. The qRT-PCR results confirmed *CREB1* overexpression or *JNK (MAPK8)* downregulation in the cells transfected with pLVX-IRES-*CREB1*-ZsGreen1 or Lenti-CAS9-*MAPK8*-Puro, respectively (mean \pm SEM, $n = 3$ biological replicates, *** $p < 0.001$).

D. *JNK (MAPK8)* overexpression significantly interrupted the effects of SP600125 on induced neuron generation. a-b, Immunofluorescence staining for TUJ1 and MAP2. c, qRT-PCR data demonstrated that *JNK* was upregulated in the cells transfected with pLVX-IRES-*MAPK8*-ZsGreen1. d, *JNK* overexpression decreased the rate of TUJ- and MAP2 positive cells under SP600125 induction. Scale bars, 200 μm . Magnification scale bars, 40 μm (means \pm SEMs, $n = 3$ biological replicates, *** $p < 0.001$).

E. *CREB1* downregulation significantly interrupted the effects of forskolin on neuronal generation. a-b, Immunofluorescence staining for TUJ1 and MAP2. c, qPCR data demonstrated that *CREB1* was downregulated in the cells transfected with Lenti-CAS9-*CREB1*-Puro. d, *CREB1* downregulation decreased the rates of TUJ- and MAP2-positive cells under forskolin induction. Scale bars, 200 μm . Magnification scale bars, 40 μm (means \pm SEMs, $n = 3$ biological replicates, *** $p < 0.001$).

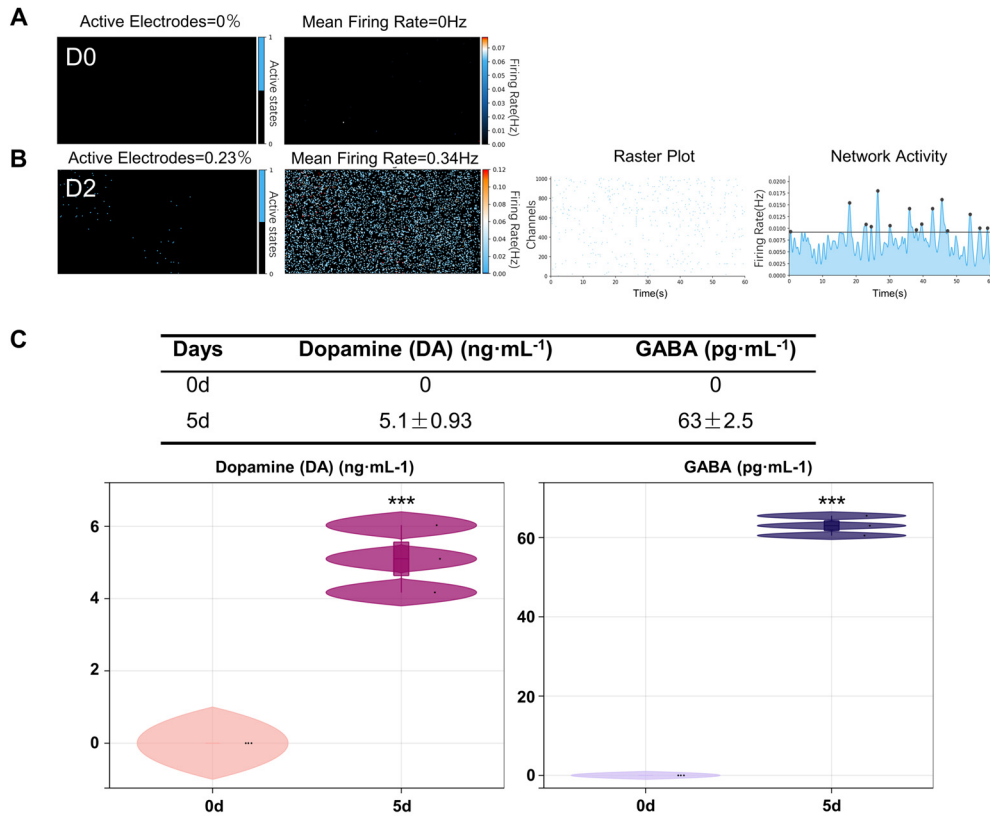


Figure S6. Electrophysiological properties of BJ cells (D0), induced cells (D2) and the neurotransmitter examination of induced neurons.

A. HD-MEA electrical images showing the 2D spatial distributions of active electrodes (%) and the mean firing rate (Hz) on day 0 (D0/BJ cells). No significant signals were detected for these negative controls (n = 3 biological replicates).

B. HD-MEA electrical images showing the spatial distributions of active electrodes (%) and the mean firing rate (Hz) on day 2 (D2). On D2, the HD-MEA chip detected the electrical signals (0.23%) of cells in each channel and the network activity (firing rate (Hz)) (0.34 Hz) with a cycle of 60 seconds (n=3 biological replicates).

C. Dopamine (DA) and GABA neurotransmitters secreted by induced cells at 0-, 5 days post forskolin induction, respectively (Unpaired t test. Two-tailed, n=3 biological replicates, ***p < 0.001).

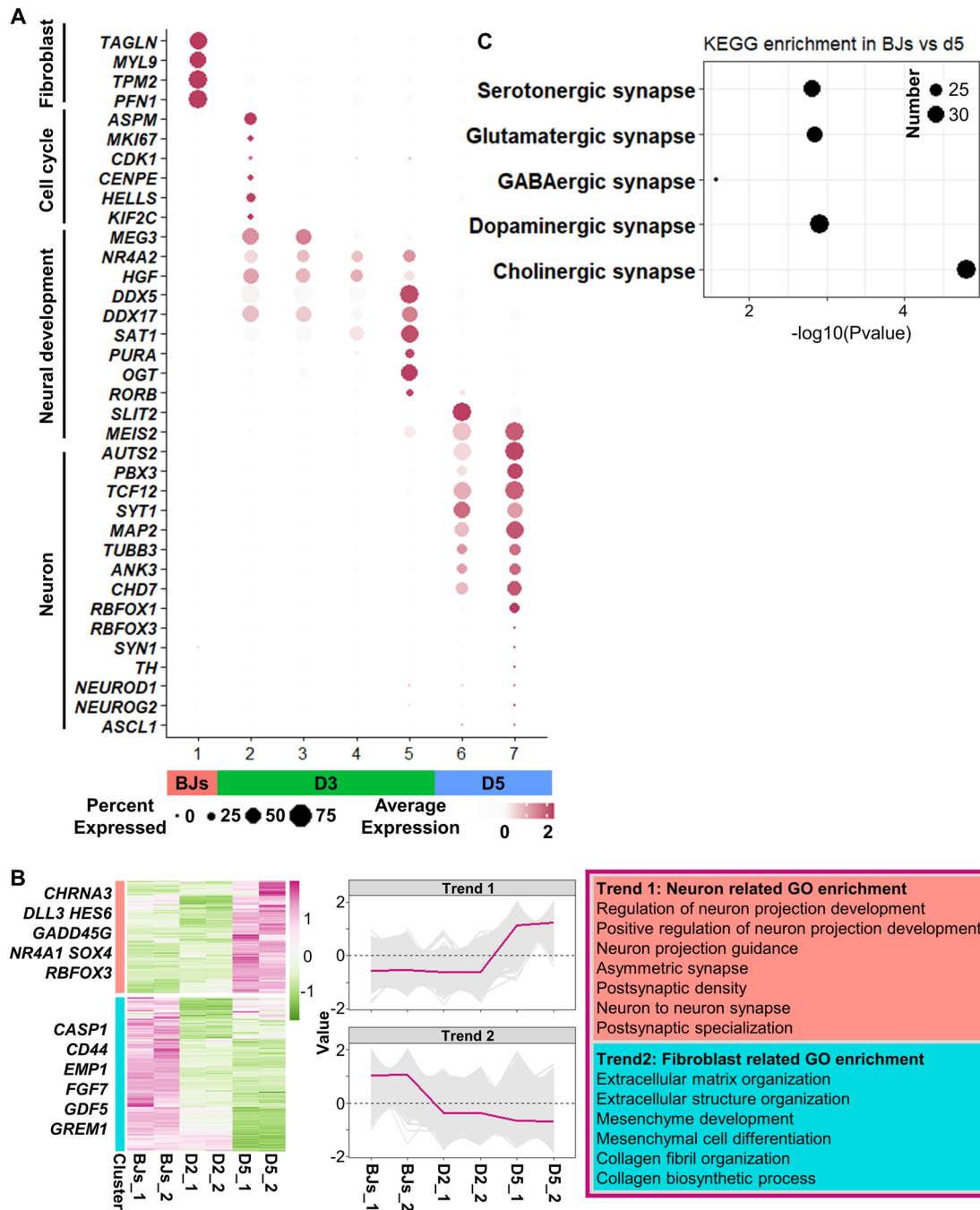


Figure S7. Bulk mRNA-seq and scRNA-seq analysis revealed the conversion of BJ cells into FiNs.

A. Dot plot of scRNA-seq data showing the expression pattern of fibroblast-, cell cycle-, neural development- and neuron-related genes in the putative trajectory.

B. Heatmap and GO enrichment of differentially expressed genes (DEGs) from the mRNA-seq data (BJ cells, days 2 and 5 (D2 and D5)). The DEGs were divided into two clusters based on their expression patterns (Trends 1 and 2). The DEGs of Trend 1 were enriched with fibroblast-related GO terms, and the DEGs of trend 2 were enriched with neuron-related GO terms.

C. KEGG enrichment analysis showed that the neuronal subtype terms were enriched in D5 cells samples.

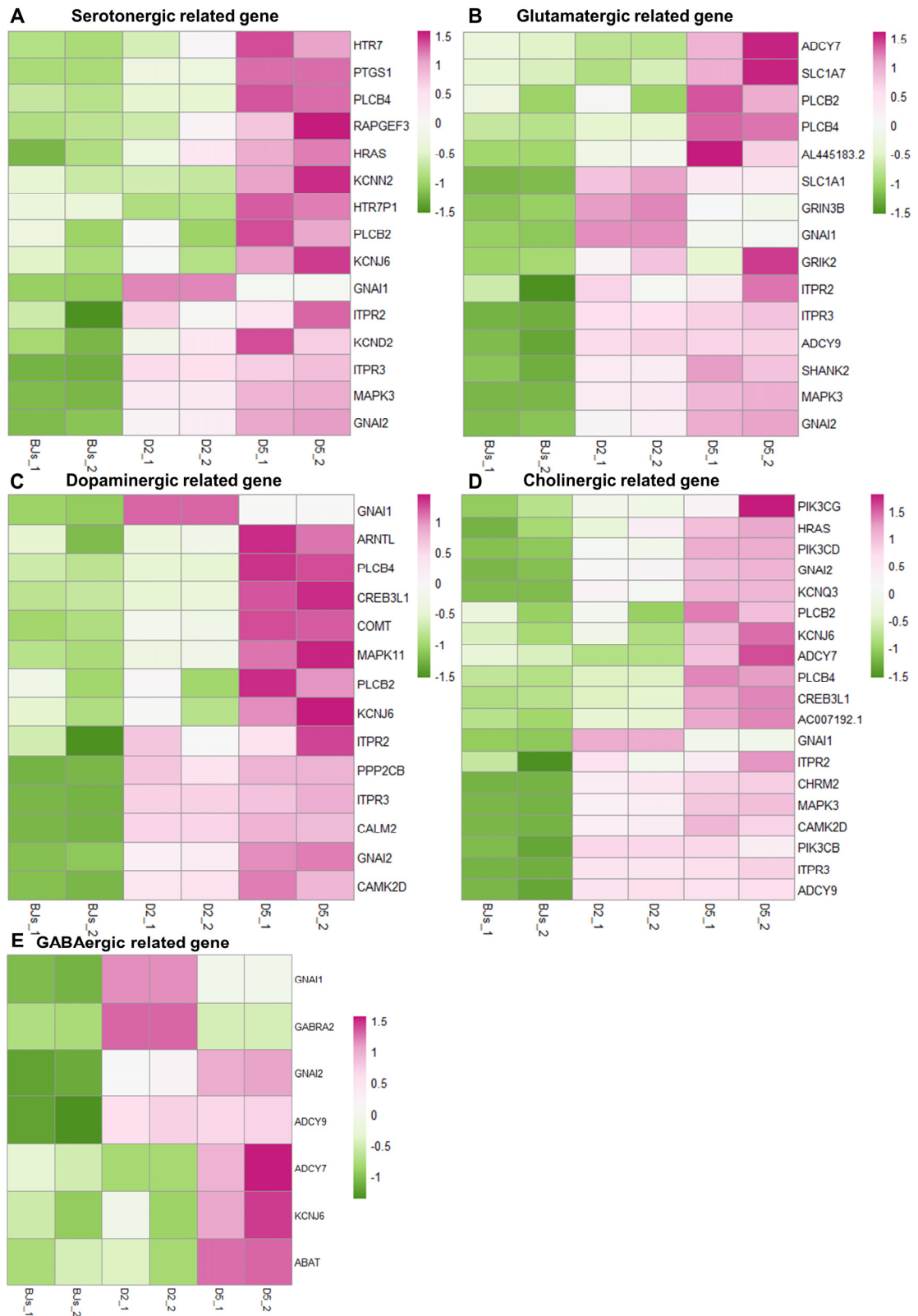


Figure S8. Heatmap shows significant upregulation of neuronal subtype genes.

A-E. Heatmap of Serotonergic related genes, Glutamatergic related genes, Dopaminergic related gene, Cholinergic related gene and GABAergic related gene showing significant upregulation during the reprogramming process.

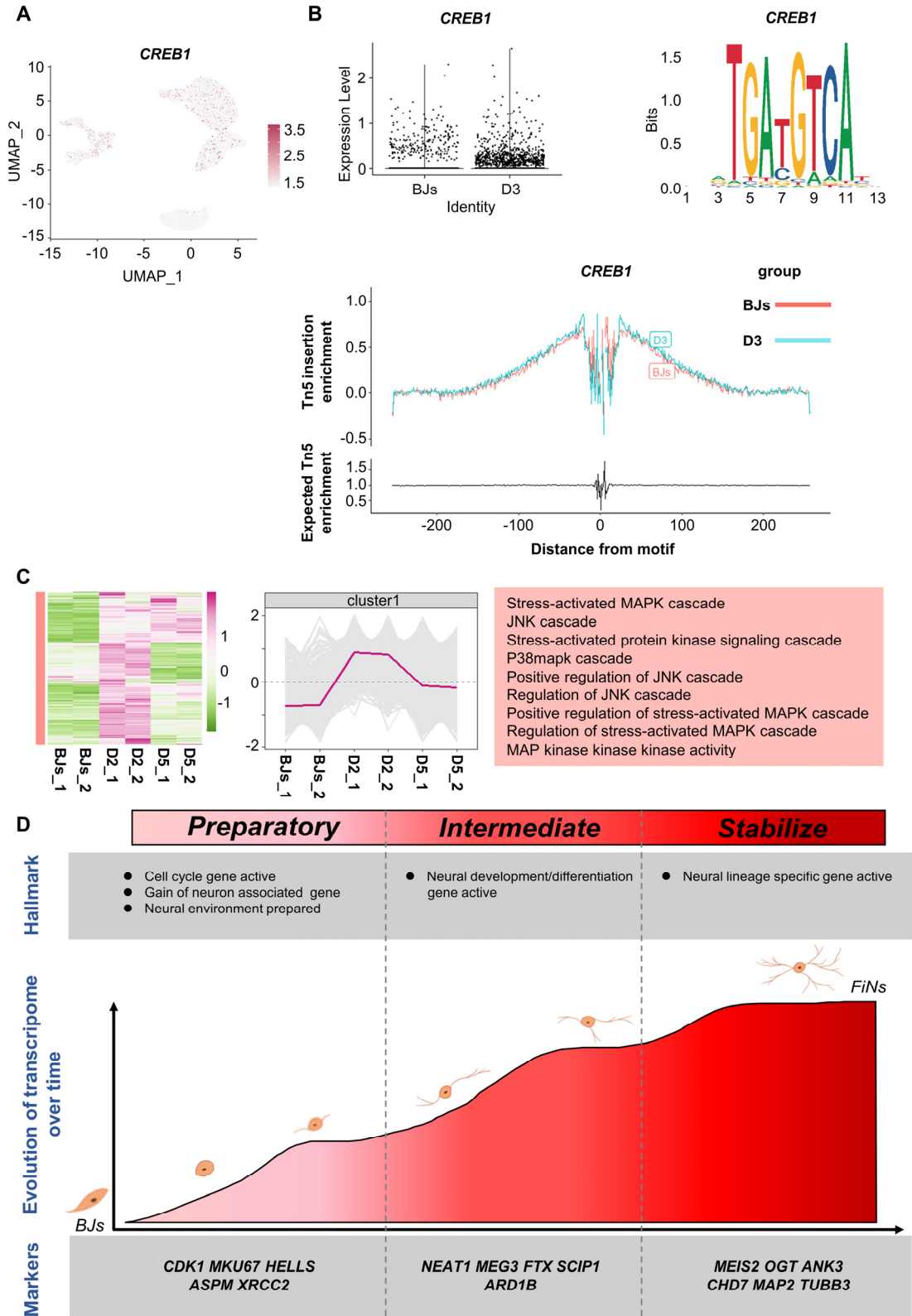


Figure S9. Single-cell sequencing (scRNA-seq and scATAC-seq) analysis revealed that *CREB1* and *JNK* play important initial roles in FiN reprogramming.

A. UMAP plot of *CREB1* expression in different clusters from the scRNA-seq data. *CREB1* is expressed under forskolin induction during the FiN reprogramming process.

B. The violin plot (left), the transcription factor (TF) footprints (right) of *CREB1* motifs, and the *CREB1 Tn5* insertion bias track (below) showed that *CREB1* was significantly enriched in the D3 cells sample in the scATAC-seq data.

C. Heatmap of DEGs in the bulk mRNA-seq data (BJ cells, day-2 and day-5 samples). The trend line is in the middle, and the GO categories are shown on the right. The results indicate that the MAPK/JNK pathway is closely involved in the early stage of FiN reprogramming.

D. Cell fate conversion model for the FiN reprogramming process. Three major states (preparatory, intermediate, and stabilized) make up the reprogramming process induced by forskolin. The schematic diagram of cell morphological changes beside the black line indicates the morphological changes that occur during each reprogramming state. Each stage's genes are presented at the bottom. The characteristics of each stage are described at the top.